2

Kinetic Analysis for Analyte–Receptor Binding and Dissociation in Biosensor Applications: a Fractal Analysis

AJIT SADANA*

Chemical Engineering Department, University of Mississippi, Post Office Box 1848, University, MS 38677-1848, U.S.A.

Introduction

To acquire an understanding of biological processes at the molecular level requires two basic approaches: structural and functional analysis. Under ideal conditions these should complement each other and provide a complete picture of the molecular processes. Electron microscopy, sequence analysis, mass spectroscopy, X-ray and electron diffraction studies are routinely employed as structural techniques. These provide information about the atomic organization of individual as well as interacting biomolecules, but these have the disadvantage of being static and 'frozen' in time. Functional investigation techniques like affinity chromatography, immunological techniques, and spectrophotometric techniques give valuable information on the conditions and the specificity of the interaction, but are (a) unable to follow a process in time, or (b) are too slow to be rendered suitable for most biospecific interactions. Moreover, these techniques demand some kind of labelling of interactants which is undesirable as it may interfere with the interaction and this will necessitate purification of the interactants in large quantities.

A promising area in the investigation of biomolecular interactions is the development of biosensors. These biosensors are finding application in the areas of biotechnology, physics, chemistry, medicine, aviation, oceanography, and environmental control. These sensors or biosensors may be utilized to monitor the analyte–receptor reactions in real time (Myszka *et al.*, 1997), besides some techniques like the surface plasmon resonance (SPR) biosensor do not require radiolabelling or biochemical tagging (Jonsson *et al.*, 1991), are reusable, have a flexible experimental

*To whom correspondence may be addressed (cmsadana@olemiss.edu)

Abbreviations: SPR, surface plasmon resonance; MS, mass spectrometry; SAMs, self-assembled monolayers; Ag, antigen; Ab, antibody; RNA, ribonucleic acid; RNAP, ribonucleic acid polymerase; argR, arginine repressor; aOF, *arg* operator fragment.

Biotechnology and Genetic Engineering Reviews – Vol. 18, July 2001
0264–8725/01/18/29–48 $20.00 + $0.00 © Intercept Ltd, P.O. Box 716, Andover, Hampshire SP10 1YG, U.K.

design, provide a rapid and automated analysis, and have a completely integrated system. Besides, the SPR in combination with mass spectrometry (MS) exhibits the potential to provide proteomic analysis (Williams and Addona, 2000).

The importance of providing a better understanding of the mode of operation of biosensors to improve their sensitivity, stability, and specificity has been emphasized. For the binding reaction to occur, one of the components has to be bound to or immobilized to the surface. This often leads to mass transfer limitations and subsequent complexities. Nevertheless, the solid-phase immunoassay technique represents a convenient method for the separation and/or detection of reactants (for example, antigen) in a solution because the binding of antigen to antibody-coated surface (or *vice versa*) is sensed directly or rapidly.

There is a need to characterize the reactions occurring at the biosensor surface in the presence of diffusional limitations that are inevitably present in these types of systems. It is essential to characterize not only the associative or binding reaction (by a binding rate coefficient, k_{bind} or k_{ads}), but also the desorption or dissociation reaction (by a desorption rate coefficient, k_{des} or k_{diss}). This significantly assists in enhancing the biosensor performance parameters, such as reusability, multiple usage for the same analyte, and stability, besides providing further insights into sensitivity, reproducibility, and specificity of the biosensor. The ratio of k_{diss} (or k_d) to k_{bind} (or k_b) (equal to K) may be used to help further characterize the biosensor–analyte–receptor system. In essence, the analysis of just the binding step is incomplete, and the analysis of the binding and the dissociation step provides a more complete picture of the analyte–receptor reaction on the surface. The details of association/dissociation of the analyte (antibody or substrate) to a receptor (antigen or enzyme) immobilized on a surface is of tremendous significance for the development of immunodiagnostic devices as well as for biosensors (Pisarchick *et al.*, 1992). The analysis to be presented is, in general, applicable to ligand–receptor and analyte–receptorless systems for biosensor and other applications (e.g. membrane–surface reactions).

External diffusional limitations play a role in the analysis of immunodiagnostic assays (Giaver, 1976; Eddowes, 1987/1988; Bluestein *et al.*, 1987; Place *et al.*, 1991; Glaser, 1993; Fischer *et al.*, 1994). The influence of diffusion in such systems has been analysed to some extent (Stenberg and Nygren, 1982; Nygren and Stenberg, 1985; Stenberg *et al.*, 1986; Place *et al.*, 1991; Sjoelander and Urbaniczky, 1991; Sadana and Sii, 1992a,b; Sadana and Madagula, 1994; Morton *et al.*, 1995; Sadana and Beelaram, 1995). The influence of partial (Christensen, 1997) and total (Matsuda, 1967; Elbicki *et al.*, 1984; Edwards *et al.*, 1995) mass transport limitations on analyte–receptor binding kinetics for biosensor applications is available. The analysis presented for partial mass transport limitation (Christensen, 1997) is applicable to simple one-to-one association as well as to cases in which there is heterogeneity of the analyte or the liquid. This applies to the different types of biosensors utilized for the detection of different analytes.

Recently, Markgren *et al.* (2000) have utilized the SPR biosensor to analyse the kinetics of interaction between HIV-1 protease and inhibitors. These authors indicate that the identification, design, synthesis and enzyme inhibitor characteristics are becoming essential in drug discovery. They emphasize that the analysis of the dissociation phase of the analyte–receptor reaction is not only required for detailed mechanistic studies, but also for evaluating equilibrium characteristics. The

dissociation rate coefficient helps the drug candidate optimization, and is of relevance as far as pharmacokinetics and pharmacodynamics are concerned. Pargellis *et al.* (1994) have also analysed the association and dissociation kinetics for the binding of inhibitors to HIV-1 protease by utilizing a novel method that employs a pair of integrated equations. These authors also emphasize that the dissociation rate coefficients are critical in the selection of a drug candidate, as lower k_d (k_{off}) values indicate longer half-lives for the inactive enzyme–inhibitor (EI) complex.

Rao *et al.* (1999) have utilized the SPR biosensor to analyse the association–dissociation of vancomycin and its dimer to self-assembled monolayers (SAMs) presenting D-Ala-D-Ala. These authors indicate the complexities involved in the kinetic analysis which includes the presence of two binding modes on the surface (monovalent and divalent forms), and mass transport limitations. Their analysis points to the similarities between binding of the analyte to the surface and in solution. They attribute that to the nature of the SAM surface. Stockley *et al.* (1998) have recently analysed the molecular details of macromolecular interactions at prokaryotic promoter–operators. They indicated that for the *Escherichia coli* methionine repressor, MetJ, there is a direct correlation for the interaction of the protein with synthetic and natural operator sites with the stoichiometry of the complexes formed.

In most of the analysis presented above, barring the few exceptions indicated, only the association or the binding of the analyte to the receptor is, in general, analysed. Apparently, up until now, the dissociation kinetics (of the analyte–receptor complex on the surface) have not been discussed or presented in great detail. One way of characterizing the dissociation kinetics is by giving the half-life ($t_{1/2}$). This is not entirely adequate. This review attempts to address this issue by analysing work – with particular reference to work in our own laboratory – concerning both the association as well as the dissociation phases of the analyte–receptor kinetics on the biosensor surface. This provides a more complete picture for the analyte–receptor biosensor system, just like an analysis of the unfolding/folding of an enzyme provides a better picture of the mechanistic reactions involved in converting an active enzyme to a deactivated one, and *vice versa*. In general, the analysis should be applicable to analyte–receptor reactions occurring on different surfaces, for example cellular surfaces.

Kopelman (1988) indicates that surface diffusion-controlled reactions that occur on clusters or islands are expected to exhibit anomalous and fractal-like kinetics. These fractal kinetics exhibit anomalous reaction orders and time-dependent (e.g. binding or dissociation) coefficients. Fractals are disordered systems with the disorder described by non-integral dimensions (Pfeifer and Obert, 1989). Kopelman (1988) further indicates that as long as surface irregularities show scale invariance that is dilatational symmetry, they can be characterized by a single number, the fractal dimension. The fractal dimension is a global property and is insensitive to structural or morphological details (Pajkossy and Nyikos, 1989). Markel *et al.* (1991) indicate that fractals are scale, self-similar mathematical objects that possess non-trivial geometrical properties. Furthermore, these investigators indicate that rough surfaces, disordered layers on surfaces, and porous objects all possess fractal structure.

A consequence of the fractal nature is a power-law dependence of a correlation function (in our case analyte–receptor complex on the surface) on a coordinate (e.g. time). This fractal nature or power-law dependence is exhibited during both the

association (or binding) and the dissociation phases. In other words, the degree of roughness or heterogeneity on the surface affects both the association or binding of the analyte to the receptor on the surface, and also the dissociation of the analyte–receptor complex on the surface. The influence of the degree of heterogeneity on the surface may affect these two phases differently. Also, since this is a temporal reaction, and presumably the degree of heterogeneity may be changing with (reaction) time, there may be two (or more) different values of the degree of heterogeneity for the association and the dissociation phases.

Fractal aggregate scaling relationships have been determined for both diffusion-limited and diffusion-limited scaling aggregation processes in spatial dimension 2,3,4 and 5 (Sorenson and Roberts, 1997). Fractal dimension values for the kinetics of antigen–antibody binding (Milum and Sadana, 1997; Sadana, 1997) and analyte–receptor binding (Sadana and Sutaria, 1997) are available. We would like to extend these ideas now to the dissociation phase as well. One would like to delineate the role of surface roughness on the speed of response, specificity, stability, sensitivity, and the regenerability or reusability of fibre-optic and other biosensors. We will obtain values of the fractal dimensions and the rate coefficient values for the association (binding) as well as the dissociation phases for the macromolecular interactions at prokaryotic promoter–operators using Stockley *et al.* (1998) data. A comparison of the values obtained for these two phases for the biosensor analysed, and for the different reaction parameters in each case should significantly assist in enhancing the relevant biosensor performance parameters. The non-integer orders of dependence obtained for the binding and dissociation rate coefficient(s) on their respective fractal dimension(s) further reinforce the fractal nature of these analyte–receptor binding/dissociation systems.

Theory

An analysis of the binding kinetics of the antigen in solution to antibody immobilized on the biosensor surface is available (Milum and Sadana, 1997). The influence of lateral interactions on the surface and variable rate coefficients is also available (Sadana and Madagula, 1993). Here we present a method of estimating fractal dimensions and rate coefficients for both the association as well as the dissociation phases for analyte–receptor systems utilized in the SPR biosensor.

VARIABLE BINDING RATE COEFFICIENT

Kopelman (1988) has indicated that classical reaction kinetics are sometimes unsatisfactory when the reactants are spatially constrained on the microscopic level by walls, phase boundaries, or force fields. Such heterogeneous reactions, e.g. bioenzymatic reactions, that occur at interfaces of different phases exhibit fractal orders for elementary reactions and rate coefficients with temporal memories. In such reactions, the rate coefficient is given by:

$$k_t = k' t^{-b} \tag{2.1}$$

In general, k_t depends on time, whereas $k' = k_t\,(t = 1)$ does not. Kopelman (1988) indicates that in three dimensions (homogeneous space), $b = 0$. This is in agreement

with the results obtained in classical kinetics. Also, with vigorous stirring, the system is made homogeneous and b again equals zero. However, for diffusion-limited reactions occurring in fractal spaces, $b > 0$; this yields a time-dependent rate coefficient.

The random fluctuations in a two-state process in ligand binding kinetics have been analysed (Di Cera, 1991). The stochastic approach can be used as a means to explain the variable binding rate coefficient. These ideas may also be extended to the dissociation rate coefficient. The simplest way to model these fluctuations is to assume that the binding (or the dissociation) rate coefficient is the sum of its deterministic value (invariant) and the fluctuation (z[t]) (Di Cera, 1991). This z(t) is a random function with a zero mean. The decreasing and increasing binding rate coefficients can be assumed to exhibit an exponential form (Cuypers *et al.*, 1987). A similar statement can also be made for the dissociation rate coefficient.

Sadana and Madagula (1993) analysed the influence of a decreasing and an increasing binding rate coefficient on the antigen concentration when the antibody is immobilized on the surface. These investigators noted that for an increasing binding rate coefficient, after a brief time interval, as time increases, the concentration of the antigen near the surface decreases, as expected for the cases when lateral interactions are present or absent. The diffusion-limited binding kinetics of antigen (or antibody or substrate) in solution to antibody (or antigen or enzyme) immobilized on a biosensor surface has been analysed within a fractal framework (Sadana, 1997; Milum and Sadana, 1997). Furthermore, experimental data presented for the binding of human immunodeficiency virus (HIV) (antigen) to the antibody anti-HIV immobilized on a surface show a characteristic ordered 'disorder' (Anderson, 1993). This indicates the possibility of a fractal-like surface. It is obvious that the above biosensor system (wherein either the antigen or the antibody is attached to the surface) along with its different complexities, including heterogeneities on the surface and in solution, diffusion-coupled reactions, and time-varying adsorption (or binding), and even dissociation rate coefficients, may be characterized as a fractal system. Havlin (1989) has briefly reviewed and discussed these results. The diffusion of reactants toward fractal surfaces has been analysed (Sadana, 1995). Here we extend the ideas to dissociation reactions as well (that is the dissociation of the analyte–receptor complex on the surface).

SINGLE-FRACTAL ANALYSIS

Binding rate coefficient

Havlin (1989) indicates that the diffusion of a particle (analyte [Ag]) from a homogeneous solution to a solid surface (e.g. receptor [Ab]-coated surface) on which it reacts to form a product (analyte–receptor complex; (Ag.Ab)) is given by:

$$(\text{Analyte.Receptor}) \sim \begin{cases} t^{(3-D_{f,\text{bind}})/2} = t^{p}(t < t_c) \\ t^{1/2}(t < t_c) \end{cases} \qquad (2.2a)$$

Here $D_{f,\text{bind}}$ is the fractal dimension of the surface during the binding step. *Equation 2.2a* indicates that the concentration of the product Ab.Ag(t) in a reaction

Ab + Ag → Ab.Ag on a solid fractal surface scales at short and intermediate time scales as [Ab.Ag] ∝ t^p with the coefficient $p = (3 - D_{f,bind})/2$ at short time scales, and $p = ½$ at intermediate time scales. This equation is associated with the short-term diffusional properties of a random walk on a fractal surface. Note that in perfectly stirred kinetics on a regular surface (nonfractal) structure (or surface), k_1 is a constant; that it is independent of time. In other words, the limit of regular structures (or surfaces) and the absence of diffusion-limited kinetics leads to k_{bind} being independent of time. In all other situations, one would expect a scaling behaviour given by $k_{bind} k' t^{-b}$ with $-b = p < 0$. Also, the appearance of the coefficient, p, different from $p = 0$ is the consequence of two different phenomena, i.e. the heterogeneity (fractality) of the surface and the imperfect mixing (diffusion-limited) condition.

Havlin (1989) indicates that the crossover value may be determined by $r_c^2 t_c$. Above the characteristic length, r_c, the self-similarity is lost. Above t_c, the surface may be considered homogeneous, since the self-similarity property disappears, and 'regular' diffusion is now present. For the present analysis, t_c is chosen arbitrarily. For the purpose of this analysis, we assume that the value of t_c is not reached. One may consider the analysis to be presented as an intermediate 'heuristic' approach in that in the future one may also be able to develop an autonomous (and not time-dependent) model of diffusion-controlled kinetics.

Dissociation rate coefficient

Similar to the binding rate coefficient, we propose that a similar mechanism is involved (except in reverse) for the dissociation step. In this case, the dissociation takes place from a fractal surface. The diffusion of the dissociated particle (receptor [Ab] or analyte [Ag])

$$(\text{Analyte.Receptor}) \sim -t^{(3-D_{f,d})/2} (t > t_d) \tag{2.2b}$$

Here $D_{f,diss}$ is the fractal dimension of the surface for the dissociation step. t_{diss} represents the start of the dissociation step. This corresponds to the highest concentration of the analyte–receptor on the surface. Henceforth, its concentration only decreases. $D_{f,bind}$ may or may not be equal to $D_{f,diss}$. *Equation 2.2b* indicates that during the dissociation step, the concentration of the product Ab.Ag(t) in the reaction Ag.Ab → Ab + Ag on a solid fractal surface scales at short and intermediate time scales as [Ab.Ag] ∝ t^p with the coefficient, p now equal to $(3 - D_{f,diss})/2$ at short time scales, and $p = ½$ at intermediate time scales. In essence, the assumptions that are applicable in the association (or binding) step are applicable for the dissociation step. Once again, this equation is associated with the short-term diffusional properties of a random walk on a fractal surface. Note that in perfectly stirred kinetics on a regular surface (nonfractal) structure (or surface), k_{diss} is a constant, that is, it is independent of time. In other words, the limit of regular structures (or surfaces) and in the absence of diffusion-limited kinetics leads to k_{diss} being independent of time. In all other situations, one would expect a scaling behaviour given by $k_{diss} = -k' t^{-b}$ with $-b = p < 0$. Once again, the appearance of the coefficient, p, different from $p = 0$ is the consequence of two different phenomena, i.e. the heterogeneity (fractality) of the surface and the imperfect mixing (diffusion-limited) condition. The ratio, K (often referred to as affinity)

$= k_{diss}/k_{bind}$, besides providing physical insights into the analyte–receptor system, is of practical importance since it may be used to help determine (and possibly enhance) the regenerability, reusability, stability, and other biosensor performance parameters.

DUAL-FRACTAL ANALYSIS

Binding rate coefficient

The single-fractal analysis we have just presented is extended to include two fractal dimensions. At present, the time ($t = t_1$) at which the first fractal dimension 'changes' to the second fractal dimension is arbitrary and empirical. For the most part it is dictated by the data analysed and the experience gained by handling a single-fractal analysis. A smoother curve is obtained in the 'transition'region, if care is taken to select the correct number of points for the two regions. In this case, the analyte–receptor complex (Ag.Ab) is given by:

$$(\text{Analyte.Receptor}) \sim \begin{cases} t^{(3-D_{f1,a})/2} = t^{p1}(t < t_1) \\ t^{(3-D_{f2,a})/2} = t^{p2}(t_1 < t < t_2 = t_c) \\ t^{1/2} = (t < t_c) \end{cases} \tag{2.2c}$$

Dissociation rate coefficient

Once again, similar to the binding rate coefficient(s), we propose that a similar mechanism is involved (except in reverse) for the dissociation step. In this case, the dissociation takes place from a fractal surface. The diffusion of the dissociated particle (receptor [Ab] or analyte [Ag]) from the solid surface (e.g. analyte [Ag]-receptor [Ab] complex coated surface) into solution may be given as a first approximation by:

$$(\text{Analyte.Receptor}) \sim \begin{cases} t^{(3-D_{f1,d})/2} = (t_d < t < t_{d1}) \\ t^{(3-D_{f2,d})/2}(t_{d1} < t < t_{d2}) \end{cases} \tag{2.2d}$$

Note that different combinations of the binding and dissociation steps are possible as far as the fractal analysis is concerned. Each of these steps or phases can be represented by either a single- or a dual-fractal analysis. For example, the binding or the association phase may be adequately described by a single-fractal analysis. Then, it is not necessary that the dissociation step should also be represented by a single-fractal analysis. It is quite possible that the dissociation step may need to be adequately described by a dual-fractal analysis. Also, the association or the binding step may be adequately described by a dual-fractal analysis. Then, the dissociation phase may be adequately described by either a single- or a dual-fractal analysis. In effect, four possible combinations are possible: single fractal (association)–single fractal (dissociation); single-fractal (association)–dual-fractal (dissociation); dual-fractal (association)–single-fractal (dissociation); dual-fractal (association)–dual-fractal (dissociation). Presumably, it is only by the analysis of a large number of association–dissociation analyte–receptor data from a wide variety of systems that this point may be further clarified.

Results

At the outset it is appropriate to indicate that a fractal analysis will be applied to the data obtained for analyte–receptor binding and dissociation data for different biosensor systems. This is one possible explanation for analysing the diffusion-limited binding and dissociation kinetics assumed to be present in all of the systems analysed. The parameters thus obtained would provide a useful comparison of different situations. Alternate expressions involving saturation, first-order reaction, and no diffusion limitations are possible, but they are apparently deficient in describing the heterogeneity that inherently exists on the surface. The analyte–receptor binding as well as the dissociation reaction is a complex reaction, and the fractal analysis via the fractal dimension (either $D_{f,bind}$ or $D_{f,diss}$) and the rate coefficient for binding (k_{bind}) or dissociation (k_{diss}) provide a useful lumped parameter(s) analysis of the diffusion-limited situation.

Also, we do not present any independent proof or physical evidence for the existence of fractals in the analysis of these analyte–receptor binding/dissociation systems except by indicating that it has been applied in other areas and that it is a convenient means to make more quantitative the degree of heterogeneity that exists on the surface. Thus, in all fairness, this is one possible way by which to analyse this analyte–receptor binding/dissociation data. One might justifiably argue that appropriate modelling may be achieved by using a Langmuirian or other approach. The Langmuirian approach has a major drawback because it does not allow for or accommodate the heterogeneity that exists on the surface.

Stockley *et al.* (1998) have utilized the surface plasmon resonance (SPR) BIACORE biosensor to analyse the molecular details of macromolecular interactions at prokaryotic promoter–operators. These authors wanted to make more quantitative and to better understand transcriptional processes. *Figure 2.1* shows the binding and dissociation of different concentrations of RNA polymerase (RNAP) in solution to *Escherichia coli metF* (methionine repressor) immobilized to an SPR biosensor surface. The *metF* operator fragment utilized contains the promoter elements recognized by RNAP. *Figure 2.1a* shows the binding and dissociation of 1.5 nM RNAP in solution to *metF* immobilized on a sensor surface. The binding (*Equation 2.2a*) and the dissociation kinetics (*Equation 2.2c*) are adequately described by a single-fractal analysis. The points are the experimental results obtained by Stockley *et al.* (1998). The solid lines are our contribution to the results. The solid line presented in the figure fits a single-fractal analysis to the experimental data. *Table 2.1* shows the values of the binding rate coefficient, k, the dissociation rate coefficient, k_d, the fractal dimension for binding, D_f, and the fractal dimension for dissociation, D_{fd}.

The values for the binding and dissociation rate coefficient(s) and the fractal dimension(s) for binding and dissociation presented in *Table 2.1* were obtained using Sigmaplot (1993) to model the experimental data using *Equation 2.2a*, wherein [analyte.receptor] = kt^p for the binding step, and [analyte.receptor] = $-k_dt^p$ for the dissociation step. The binding and the dissociation rate coefficient values presented in *Table 2.1* are within 95% confidence limits. For example, for the binding of 1.5 nM RNA polymerase in solution to *metF* immobilized on a sensor chip, the binding rate coefficient, k, value is 6.54 ± 0.23. The 95% confidence value indicates that 95% of the k values will lie between 6.31 and 6.77. This indicates that the values are precise and significant. The curves presented are theoretical curves.

Table 2.1. Fractal dimensions and binding, dissociation, and affinity rate coefficients for the binding and dissociation of different concentrations of RNA polymerase in solution to *metF* immobilized to a surface plasmon resonance biosensor surface (Stockley *et al.*, 1998). See text for explanation of symbols

RNA Polymerase concentration in solution, nM	k	D_f	k_d	D_{fd}	$K=k_d/k$
1.5	6.54 ± 0.23	1.59 ± 0.05	7.15 ± 0.61	1.99 ± 0.07	1.09
2.0	7.34 ± 0.33	1.56 ± 0.07	10.6 ± 0.53	2.00 ± 0.04	1.45
2.5	14.5 ± 0.61	1.76 ± 0.06	17.1 ± 0.78	2.10 ± 0.4	1.18
3.5	29.4 ± 1.36	1.93 ± 0.07	32.6 ± 1.5	2.19 ± 0.04	1.11
4.5	45.4 ± 2.31	2.03 ± 0.08	35.7 ± 1.73	2.14 ± 0.04	0.787

Figures 2.1b,c,d, and *e* show the binding of 2.0, 2.5, 3.5, and 4.5 nM RNAP in solution to *metF* immobilized on a sensor chip surface. A single-fractal analysis is sufficient to adequately describe the binding and the dissociation kinetics for each of these cases. See *Figures 2.1b–e*. The values for the binding and the dissociation rate coefficients are given in *Table 2.1*. It is of interest to note that, in general, an increase in the RNAP concentration in solution leads to increases in the rate coefficient and in the fractal dimension values in the binding and in the dissociation phases. For example, an increase in the RNAP concentration in solution from 2.0 to 2.5 nM leads to an increase in the fractal dimension for binding, D_f by 12.8% from a value of 1.56 to 1.76, and to an increase in the binding rate coefficient, k value by 97.5% (almost double) from a value of 7.34 to 14.5. Also, an increase in the RNAP concentration in solution from 2.0 to 2.5 nM leads to an increase in the fractal dimension for dissociation, D_{fd} by 5% from a value of 2.0 to 2.10, and to an increase in the rate coefficient for dissociation, k_d by 61.3% from a value of 10.6 to 17.1. Apparently, an increase in the heterogeneity on the surface (increase in the fractal dimension in either the binding or the dissociation phases) leads to increases in the rate coefficient for binding and dissociation. Similarly, an increase in the analyte (RNAP) concentration in solution also leads to increases in the rate coefficient for binding and dissociation.

Table 2.1 also shows the estimated values of the affinity, K ($=k_d/k_b$). Apparently, the highest value of K is obtained at a RNAP concentration value of 2.0 nM. Thus, if affinity is of concern, then one should utilize 2 nM RNAP concentration in solution. At RNAP concentrations higher than 2 nM, the affinity, K gradually decreases. Note that as the RNAP concentration in solution increases by a factor of 2.5 from 2.0 to 4.5 nM, the affinity K value decreases by 45.7% from a value of 1.45 to 0.787.

Figure 2.2a shows the increase in the binding rate coefficient, k with an increase in the RNAP concentration in solution. In the RNAP concentration range analysed, k is given by:

$$k = (2.53 \pm 0.511)\,[\text{RNAP}]^{1.91 \pm 0.21} \tag{2.3a}$$

Figure 2.2a shows that the fit is very reasonable. More data points would more firmly establish this equation. The binding rate coefficient, k is quite sensitive to the RNAP concentration in solution as noted by the almost second-order dependence of k on RNAP concentration. The fractional order of dependence of k on RNAP concentration (as indicated by the exponent value) reinforces the fractal nature of the system.

Figure 2.2b shows the increase in the dissociation rate coefficient, k_d with an

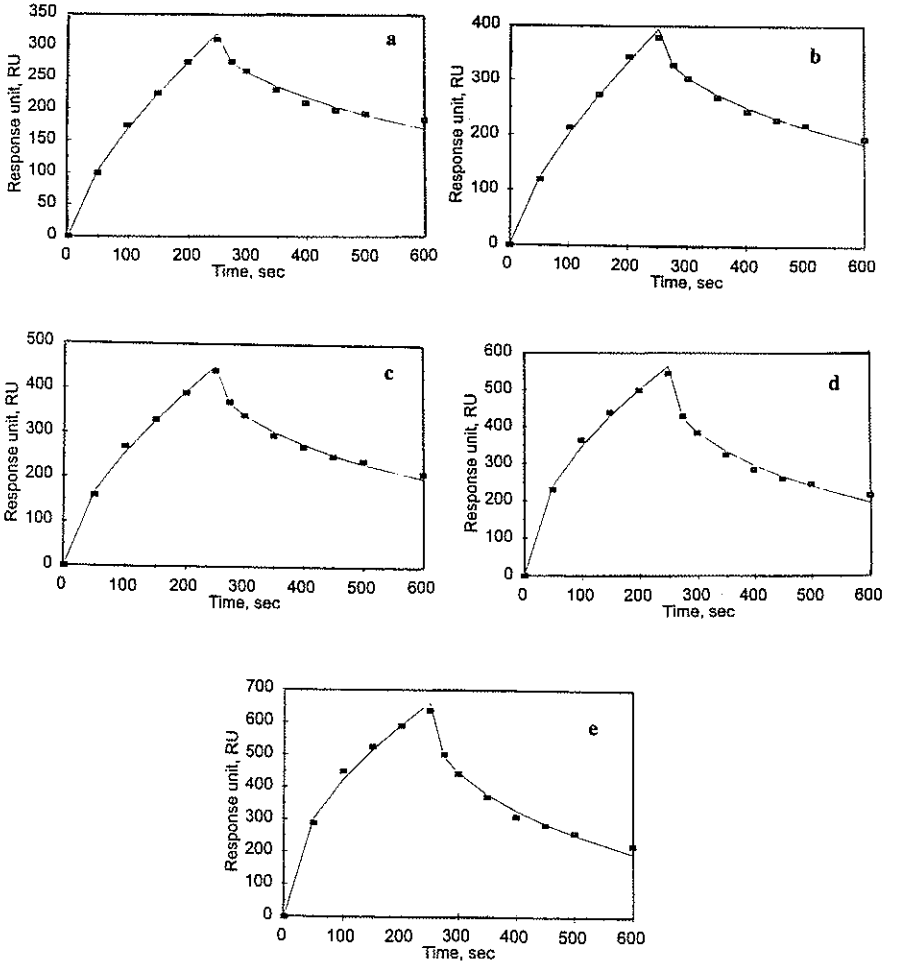

Figure 2.1. Binding and dissociation of different concentrations (in nM) of RNA polymerase (RNAP) in solution to *Escherichia coli metF* (methionine repressor) immobilized to a surface plasmon resonance biosensor surface (Stockley *et al.*, 1998): (a) 1.5 (b) 2.0 (c) 2.5 (d) 3.5 (e) 4.5.

increase in the RNAP concentration in solution. In the RNAP concentration range analysed, k_d is given by:

$$k_d = (3.83 \pm 0.55)\,[\mathrm{RNAP}]^{1.57 \pm 0.16} \tag{2.3b}$$

Figure 2.2b shows that the fit is reasonable. More data points would more firmly establish this equation. The dissociation rate coefficient is quite sensitive to the RNAP concentration in solution, as noted by the dependence of k_d on RNAP. The fractional order of dependence of k_d on RNAP (as indicated by the exponent value) reinforces the fractal nature of the system.

Figure 2.2c shows the increase in the fractal dimension, D_f during the binding phase

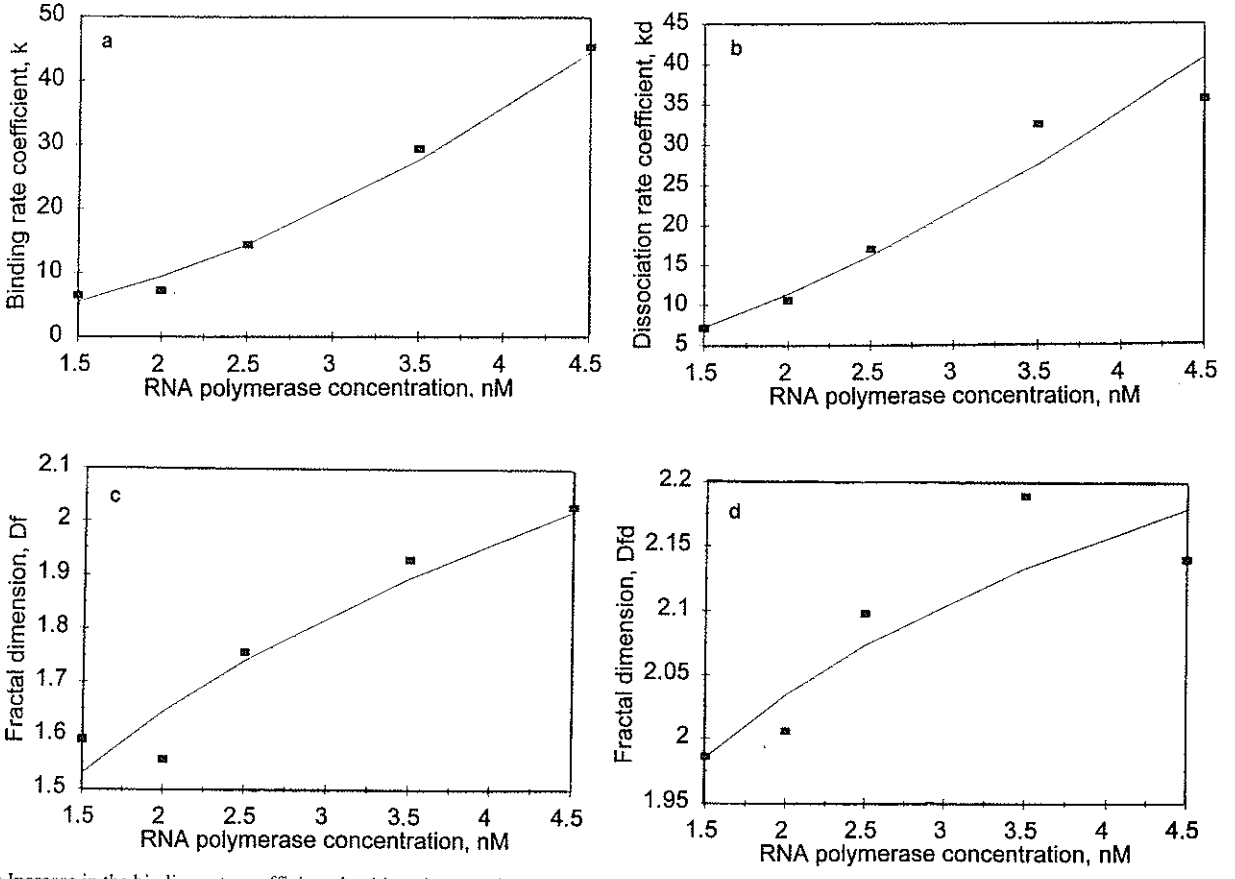

Figure 2.2. (a) Increase in the binding rate coefficient, k with an increase in the RNA polymerase concentration in solution; (b) increase in the dissociation rate coefficient, k_d with an increase in the RNA polymerase concentration in solution; (c) increase in the fractal dimension for binding, D_f with an increase in the RNA polymerase concentration in solution; (d) increase in the fractal dimension for dissociation, D_{fd} with an increase in the RNA polymerase concentration in solution.

with an increase in the RNAP concentration in solution. In the RNAP concentration range analysed, D_f is given by:

$$D_f = (1.38 \pm 0.06)\,[\text{RNAP}]^{0.25 \pm 0.05} \tag{2.3c}$$

Figure 2.2c shows that the fit is very reasonable. More data points would more firmly establish this equation. The fractal dimension for binding, D_f is only mildly sensitive to the RNAP concentration in solution as noted by the low value of the exponent. The fractional order of dependence of D_f on RNAP concentration (as indicated by the exponent value) reinforces the fractal nature of the system.

Figure 2.2d shows the increase in the fractal dimension, D_{fd} during the dissociation phase with an increase in the RNAP concentration in solution. In the RNAP concentration range analysed, D_{fd} is given by:

$$D_{fd} = (1.92 \pm 0.04)\,[\text{RNAP}]^{0.09 \pm 0.02} \tag{2.3d}$$

Figure 2.2d shows that the fit is somewhat reasonable. There is some scatter in the data. More data points are required to more firmly establish this equation. The fractal dimension, D_{fd} is only very slightly sensitive to the RNAP concentration in solution as noted by the very low dependence of D_{fd} on RNAP concentration in solution.

Figure 2.3a shows that an increase in the fractal dimension, D_f during the binding phase leads to an increase in the binding rate coefficient, k. In the 1.5 to 4.5 nM RNAP concentration range analysed, the binding rate coefficient, k is given by:

$$k = (0.26 \pm 0.03)\,D_f^{7.23 \pm 0.52} \tag{2.4a}$$

The fit is very reasonable. More data points would more firmly establish this equation. The binding rate coefficient is very sensitive to the degree of heterogeneity (D_f) on the surface, as noted by the very high value of the exponent.

Figure 2.3b shows that an increase in the fractal dimension, D_{fd} during the dissociation phase leads to an increase in the dissociation rate coefficient, k_d. In the 1.5 to 4.5 nM RNAP concentration range analysed, the dissociation rate coefficient, k_d is given by:

$$k_d = (0.00014 \pm 00004)D_{fd}^{16.0 \pm 2.75} \tag{2.4b}$$

The fit is quite reasonable. More data points are required to more firmly establish this equation. The dissociation rate coefficient, k_d is very sensitive to the degree of heterogeneity on the surface (D_{fd}) as noted by the extremely high value of the exponent. On comparing *Equations 2.4a* and *2.4b*, one notes that the dissociation rate coefficient, k_d is much more sensitive than the binding rate coefficient, k on the degree of heterogeneity that exists on the surface. Note also that for all of the cases presented in *Table 2.1*, the fractal dimension for the dissociation phase, D_{fd} is always higher than its corresponding value in the binding phase, D_f.

Stockley *et al.* (1998) have also analysed the influence of different concentrations of different *arg* operator fragments (aOF) in the absence of L-arginine in solution on their binding to arginine repressors (argR) immobilized on a surface plasmon resonance (SPR) biosensor surface. *Figure 2.4a* shows the binding and dissociation of 5 nM of the *arg* operator, *rocA* in the absence of L-arginine in solution to arginine repressors (argR) immobilized on a SPR biosensor surface. A dual-fractal analysis is required to adequately describe the binding kinetics. The dissociation kinetics may be

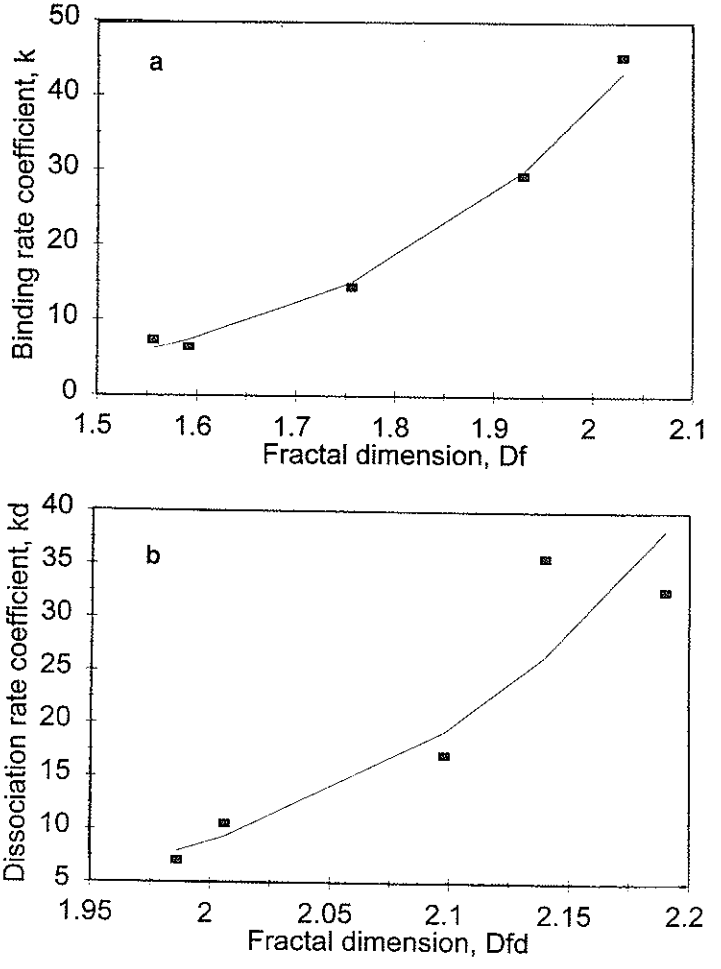

Figure 2.3. (a) Increase in the binding rate coefficient, k with an increase in the fractal dimension for binding, D_f; (b) increase in the dissociation rate coefficient, k_d with an increase in the fractal dimension for dissociation, D_{fd}.

adequately described by a single-fractal analysis. The values of the binding and the dissociation rate coefficients, as well as the fractal dimension values obtained during the binding and in the dissociation phases, are given in *Table 2.2*. In order to conserve space and to get all the columns in the table, the subscripts have been shortened. For example, k_{bind} is represented as k_b, and k_{diss} as k_d, etc. In this case, there is a change in the binding mechanism since a dual-fractal analysis is required to adequately describe the binding kinetics. It is of interest to note that for the dual-fractal analysis case during the binding phase, as the fractal dimension increases by 24.9% from $D_{f1,b}$ equal to 2.25 to 2.81, the binding rate coefficient increases by a factor of 2.74 from a value of $k_{1,b}$ equal to 2.24 to 6.13. In other words, an increase in the degree of heterogeneity on the surface (increase in the fractal dimension value) leads to an increase in the binding rate coefficient value. Since the single-fractal analysis does not describe the binding kinetics adequately, it is not analysed further.

Table 2.2. Fractal dimensions and binding and dissociation rate coefficients for the binding and dissociation of different concentrations of different *arg* operator fragments (aOF) in the absence of L-arginine in solution to arginine repressors (argR) immobilized on a surface plasmon resonance biosensor surface (Stockley *et al.*, 1998). See text for explanation of symbols

aOF concentration	k_b	$k_{1,b}$	$k_{2,b}$	k_d	$k_{d1,d}$	$k_{d2,d}$	$D_{f,b}$	$D_{f1,b}$	$D_{f2,b}$	$D_{f,d}$	$D_{f,d1}$	$D_{f,d2}$
rocA, 5 nM	2.92 ± 0.18	2.24 ± 0.07	6.13 ± 0.07	0.34 ± 0.02	na	na	2.43 ± 0.07	2.25 ± 0.06	2.81 ± 0.05	1.08 ± 0.14	na	na
rocA, 100 nM	4.04 ± 0.16	na	na	0.27 ± 0.03	na	na	2.48 ± 0.04	na	na	0.94 ± 0.19	na	na
argC, 5 nM	0.938 ± 0.01	na	na	0.307 ± 0.02	na	na	1.02 ± 0.1	na	na	1.32 ± 0.06	na	na
argC, 100 nM	1.94 ± 0.25	1.44 ± 0.22	3.88 ± 0.04	0.470 ± 0.03	na	na	2.23 ± 0.10	1.97 ± 0.21	2.59 ± 0.04	1.62 ± 0.07	na	na
ArgR 50 nM	2.70 ± 0.69	2.02 ± 0.57	7.50 ± 0.19	0.01 ± 0.00	0.036 ± 0.00	(6.00±0.04)E-05	2.17 ± 0.33	1.88 ± 0.51	2.84 ± 0.06	0.0 + 0.34	1.0 ± 0.24	0.0 ± 0.40
ArgR 100 nM	3.19 ± 0.65	2.21 ± 0.56	8.86 ± 0.00	0.012 ± 0.00	0.023 ± 0.00	(5.0±1.0)E-04	2.17 ± 0.23	1.81 ± 0.47	2.80 ± 0.00	0.00 ± 0.22	0.34 ± 0.03	0.0 + 0.62

na, not applicable.

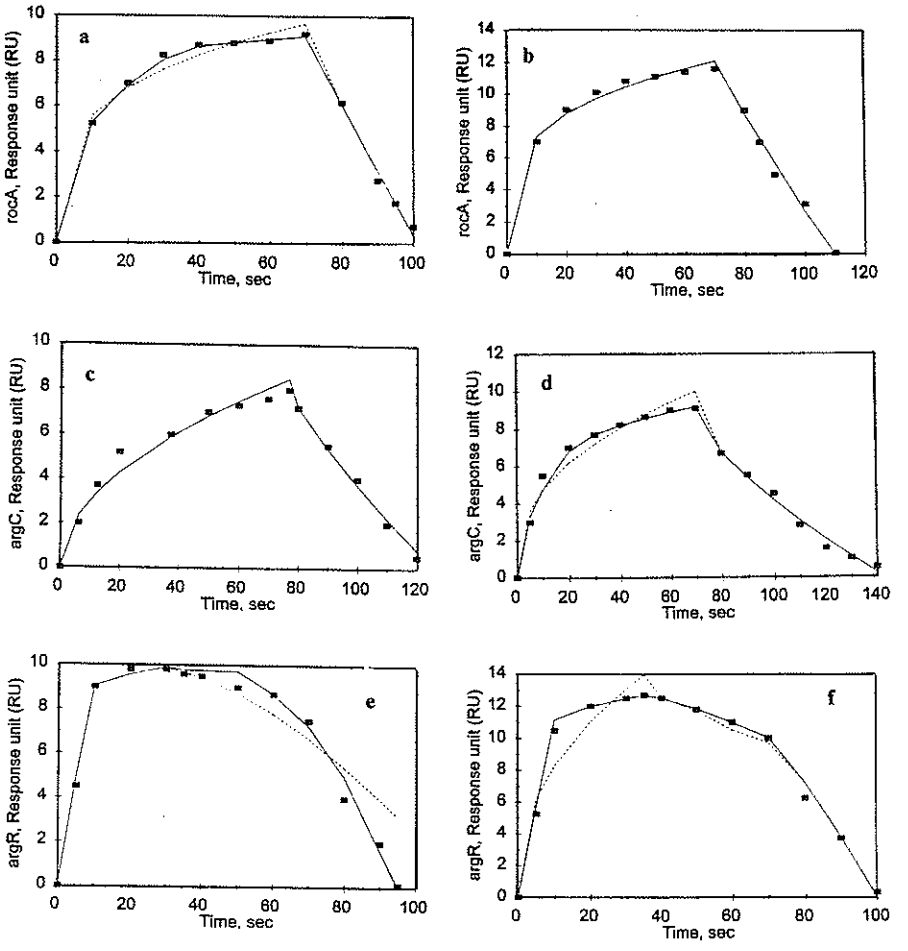

Figure 2.4. Binding and dissociation of different concentrations of different *arg* operator fragments (aOF) in the absence of L-arginine in solution to arginine repressors (ArgR) immobilized on a surface plasmon resonance biosensor surface (Stockley *et al.*, 1998). (a) 5 nM *rocA*; (b) 100 nM *rocA*; (c) 5 nM *argC*; (d) 100 nM *argC*; (e) 50 nM *argR*; (f) 100 nM *argR* (····· single-fractal analysis; —— dual-fractal analysis).

Figure 2.4b shows the binding and dissociation of 100 nM of *rocA* in the absence of L-arginine in solution to the arginine repressor (argR) immobilized on a SPR biosensor surface. In this case, a single-fractal analysis is required to adequately describe both the binding as well as the dissociation kinetics. This is of interest especially for the binding phase, since an increase in the *rocA* concentration from 5 to 100 nM leads to change in the binding mechanism. This is because the binding of 5 nM of *rocA* in solution requires a dual-fractal analysis to adequately describe the kinetics, whereas the binding of 100 nM of *rocA* in solution may be adequately described by a single-fractal analysis.

Figure 2.4c shows the binding and dissociation of 5 nM *argC* in the absence of L-arginine in solution to the arginine repressor (argR) immobilized on an SPR biosensor surface. A single-fractal analysis is required to adequately describe both the binding

and the dissociation kinetics. The values of the rate coefficients and the fractal dimensions obtained for the binding and the dissociation phases are given in *Table 2.2*. *Figure 2.4d* shows the binding and dissociation of 100 nM *argC* in the absence of L-arginine in solution to the arginine repressor (argR) immobilized on an SPR biosensor surface. In this case, a dual-fractal analysis is required to adequately describe the binding kinetics. The dissociation kinetics is adequately described by a single-fractal analysis. The values of the rate coefficient and the fractal dimensions for the binding and the dissociation phase are given in *Table 2.2*. It is of interest to note that as one goes from 5 nM to100 nM *argC* in solution the binding is adequately described by a single- and a dual-fractal analysis, respectively. This indicates that there is a change in the binding mechanism as one increases the *argC* concentration in solution from 5 to 100 nM. For both of these concentrations, dissociation kinetics are adequately described by a single-fractal analysis. In this case, an increase in the analyte concentration by a factor of 20 from 5 to 100 nM *argC* does not lead to a change in the dissociation mechanism. Thus, it is possible to have a change in the binding mechanism and no change in the dissociation mechanism, at least for this case. Note also that as one goes from the 5 to the 100 nM *argC* in solution the fractal dimension for dissociation, D_{fd} increases by 22.7% from a value of 1.32 to 1.62, and the dissociation rate coefficient, k_d increases by 32.6 % from a value of 0.307 to 0.470. An increase in the degree of heterogeneity on the surface (increase in the D_{fd} value) leads to an increase in the dissociation rate coefficient.

Figure 2.4e shows the binding and dissociation of 50 nM *argR* in the absence of L-arginine in solution to the arginine repressor (argR) immobilized on an SPR biosensor surface. A dual-fractal analysis is required to adequately describe both the binding as well as the dissociation kinetics. The values of the rate coefficients for binding and dissociation phases for both the single- and the dual-fractal analysis are given in *Table 2.2*. To avoid cluttering up the figure, curves presenting only the dual-fractal analysis for binding, and the single- and dual-fractal analysis for dissociation are shown. In this case, note that a dual-fractal analysis is required to describe both the binding and the dissociation phases. This indicates that, in this case, not only are complexities involved in the binding phase, but also during the dissociation phase. *Figure 2.4f* shows the binding and dissociation of 100 nM *argR* in the absence of L-arginine in solution to the arginine repressor (argR) immobilized on an SPR biosensor surface. Once again, a dual-fractal analysis is required to adequately describe both the binding as well as the dissociation kinetics. The values of the rate coefficients for binding and dissociation phases for both the single- and the dual-fractal analysis are given in *Table 2.2*. It is of interest to note that as one goes from the 50 to the 100 nM *argR* in solution, the fractal dimension for dissociation for the dual-fractal analysis ($D_{f,d1}$) decreases by 66% from a value of 1.0 to 0.34, and this leads to a corresponding decrease in the dissociation rate coefficient, $k_{d1,d}$ by about 36.1% from a value of 0.036 to 0.023.

Concluding remarks

A fractal analysis of the binding of an analyte in solution to a receptor immobilized on the biosensor surface provides a quantitative indication of the state of disorder (fractal dimension, $D_{f,bind}$) and the binding rate coefficient, k_{bind} on the surface. In addition, fractal dimensions for the dissociation step, $D_{f,diss}$ and dissociation rate coefficients,

k_{diss} are also presented. This provides a more complete picture of the analyte–receptor reactions occurring on the surface on comparing with an analysis of the binding step alone, as done previously (Sadana, 1999). Besides, one may also use the numerical values for the rate coefficients for binding and the dissociation steps to classify the analyte–receptor biosensor system as, for example, (a) moderate binding, extremely fast dissociation, (b) moderate binding, fast dissociation, (c) moderate binding, moderate dissociation, (d) moderate binding, slow dissociation, (e) fast binding, extremely fast dissociation, (f) fast binding, fast dissociation, (g) fast binding, moderate dissociation, and (h) fast binding, slow dissociation.

The fractal dimension value provides a quantitative measure of the degree of heterogeneity that exists on the surface for the analyte–receptor systems. The degree of heterogeneity for the binding and the dissociation phases is, in general, different for the same reaction. This indicates that the same surface exhibits two degrees of heterogeneity for the binding and the dissociation reaction. Both types of examples are given wherein either a single- or a dual-fractal analysis is required to adequately describe the binding kinetics. The dual-fractal analysis was used only when the single-fractal analysis did not provide an adequate fit. This was done by the regression analysis provided by Sigmaplot (1993). The dissociation step was adequately described by either a single-fractal or a dual-fractal analysis for the examples presented.

In accord with the prefactor analysis for fractal aggregates (Sorenson and Roberts, 1997), quantitative (predictive) expressions are developed for (a) the binding rate coefficient, k_{bind} as a function of the fractal dimension for binding, $D_{f,bind}$ for a single-fractal analysis, and for (b) the dissociation rate coefficient, k_{diss} as a function of the fractal dimension for dissociation, $D_{f,diss}$ for a single-fractal analysis. The parameter, K ($= k_d/k_b$) values presented are of interest since they provide an indication of the stability, reusability, and regenerability of the biosensor. Also, depending on one's final goal, a higher or a lower K value may be beneficial for a particular analyte–receptor system.

The fractal dimension for the binding or the dissociation phase, $D_{f,bind}$ or $D_{f,\,diss}$, respectively, is not a typical independent variable, such as analyte concentration, that may be directly manipulated. It is estimated from *Equations 2.2a* and *2.2b*, and one may consider it as a derived variable. Predictive relationships for (a) the fractal dimensions, D_f and $D_{f,d}$ and for (b) the binding (k_b) and the dissociation (k_d) rate coefficients as a function of the analyte concentration are also presented. The predictive relationships developed for (a) the binding rate coefficient as a function of the fractal dimension, and for (b) the dissociation rate coefficient as a function of the fractal dimension are of considerable value because they directly link the binding or the dissociation rate coefficient to the degree of heterogeneity that exists on the surface, and provide a means by which the binding or the dissociation rate coefficient may be manipulated by changing the degree of heterogeneity that exists on the surface. Note that a change in the degree of heterogeneity on the surface would, in general, lead to changes in both the binding and the dissociation rate coefficient. Thus, this may require a little thought and manipulation. The binding and the dissociation rate coefficients are rather sensitive to their respective fractal dimensions or the degree of heterogeneity that exists on the biosensor surface. This may be noted by the high orders of dependence. It is suggested that the fractal surface (roughness) leads to turbulence, which enhances mixing, decreases diffusional limitations, and leads to an

increase in the binding rate coefficient (Martin *et al.*, 1991), and in our case to an increase in the dissociation rate coefficient as well.

More of these studies are required to determine whether the binding and the dissociation rate coefficient are sensitive to their respective fractal dimensions or the degree of heterogeneity that exists on the biosensor surface. If this is correct, then experimentalists may find it worth their effort to pay a little more attention to the nature of the surface, and how it may be manipulated to control the relevant parameters and biosensor performance in desired directions. This would also facilitate insights into the analyte–receptor reactions occurring on the cellular surface.

References

ANDERSON, J. (1993). Unpublished results. NIH panel meeting, Case Western Reserve University, Cleveland, Ohio.

BLUESTEIN, R.C., DIACO, R., HUTSON, D.D., MILLER, W.K., NEELKANTAN, N.V., PANKRATZ, T.J., TSENG, S.Y. AND VICKERY, E.K. (1987). Application of novel chromium dioxide particles to immunoassay development. *Clinical Chemistry* **33** (9), 1543–1547.

CHRISTENSEN, L.L.H. (1997). Theoretical analysis of protein concentration determination using biosensor technology under conditions of partial mass transport limitation. *Analytical Biochemistry* **249**, 153–164.

CUYPERS, P.A., WILLEMS, G.M., KOP, J.M., CORSEL, J.W., JANSEN, M.P. AND HERMANS, W.T. (1987). In: *Proteins at interfaces: physicochemical and biochemical studies.* Eds. J.L. Brash and T.A. Horbett, pp 208–215. Washington DC: American Chemical Society.

DI CERA, E. (1991). Stochastic linkage: effect of random fluctuations on a two-state process. *Journal of Chemical Physics* **95**, 5082–5086.

EDDOWES, E. (1987/1988). Direct immunochemical sensing: basic chemical principles and fundamental limitations. *Biosensors* **3**, 1–15.

EDWARDS, P.R., GILL, A., POLLARD-KNIGHT, D.V., HOARE, M., BUCKE, P.E., LOWE, P.A. AND LEATHERBARROW, R.J. (1995). Kinetics of protein–protein interactions at the surface of an optical biosensor. *Analytical Biochemistry* **231**, 210–217.

ELBICKI, J.M., MORGAN, D.M. AND WEBER, S.G. (1984). Theoretical and practical implications on the optimization of amperometric detectors. *Analytical Chemistry* **56**, 978–985.

FISCHER, R.J., FIVASH, M., CASA-FINET, J., BLADEN, S. AND MCNITT, K.L. (1994). Real time BIA core measurements of *Escherichia coli* single stranded DNA binding (SSB) protein to polydeoxythymidylic acid reveal single-state kinetics with steric cooperativity. *Methods* **6**, 121–133.

GIAVER, I. (1976). Visual detection of carcinoembryonic antigen on surfaces. *Journal of Immunology* **116**, 766–771.

GLASER, R.W. (1993). Antigen–antibody binding and mass transport by convection and diffusion to a surface: a two-dimensional computer model of binding and dissociation kinetics. *Analytical Biochemistry* **213**, 152–158.

HAVLIN, S. (1989). Molecular diffusion and reactions. In: *The fractal approach to heterogeneous chemistry: surfaces, colloids, polymers.* Ed. D. Avnir, pp 251–269. New York: J. Wiley & Sons.

JONSSON, U., FAGERSTAM, L., IVARSSON, B., JOHNSSON, B., KARLSSON, R., LUNDH, K., LOFAS, S., PERSSON, B., ROOS, H. AND RONNBERG, I. (1991). Real-time biospecific interaction analysis using surface plasmon resonance and a sensor chip technology. *Biotechniques* **11**, 620.

KOPELMAN, R. (1988). Fractal reaction kinetics. *Science* **241**, 1620–1626.

MARKEL, V.A., MURATOV, L.S., STOCKMAN, M.I. AND GEORGE, T.F. (1991). *Physical Review B* **43** (10), 8183–81195.

MARKGREN, P.O., HAMALEINEN, M. AND DANIELSON, H. (2000). Kinetic analysis of the interaction between HIV-1 protease inhibitors using optical biosensor techniques. *Analytical Biochemistry* **279**, 71–78.

MARTIN, S.J., GRANSTAFF, V.E. AND FRYE, G.C. (1991). Effect of surface roughness on the

response of thickness-shear mode resonators in liquids. *Analytical Chemistry* **65**, 2910–2922.

MATSUDA, H. (1967). The theory of steady-state current potential curves of redox electrode reactions in hydrodynamic voltametry. II. Laminar pipe and channel flows. *Journal of Electroanalytical Chemistry* **15** (4), 325–336.

MILUM, J. AND SADANA, A. (1997). Influence of different parameters on a dual-fractal analysis for antigen–antibody binding kinetics. *Journal of Colloid and Interface Science* **187**, 128–138.

MORTON, T.A., MYSZKA, D.G. AND CHAIKEN, I.M. (1995). Interpreting complex binding kinetics from optical biosensors: a comparison of analysis by linearization, the integrated rate equation, and numerical integration. *Analytical Biochemistry* **227**, 176–185.

MYSZKA, D.G., MORTON, T.A., DOYLE, M.L. AND CHAIKEN, I.M. (1997). Kinetic analysis of a protein antigen–antibody interaction limited by mass transfer on an optical biosensor. *Biophysical Chemistry* **64**, 127–137.

NYGREN, H. AND STENBERG, M. (1985). Kinetics of antibody binding to surface-immobilized antigen: influence of mass transport on the enzyme-linked immunosorbent assay (ELISA). *Journal of Colloid and Interface Science* **107** (2), 560–568.

PAJKOSSY, T. AND NYIKOS, L. (1989). Diffusion to fractal surfaces. II. Verification of theory. *Electrochimica Acta* **34** (2), 71–179.

PARGELLIS, C.A., MORELOCK, M.M., GRAHAM, E.T., KINKADE, P., PAR, S., LUBBE, K., LAMARRE, D. AND ANDERSON, P.C. (1994). Determination of kinetic rate constants for the binding of inhibitors to HIV-1 protease and for the association and dissociation of active homodimer. *Biochemica* **33**, 12527–12534.

PFEIFER, P. AND OBERT, M. (1989). Fractals: basic concepts and terminology. In: *The fractal approach to heterogeneous chemistry: surfaces, colloids, polymers*. Ed. D. Avnir, pp 11–43. New York: J. Wiley & Sons.

PISARCHICK, M.L., GESTY, D. AND THOMPSON, N.L. (1992). Binding kinetics of an anti-nitrophenyl monoclonal fab on supported phospholipid monolayers measured by total internal reflection with photobleaching recovery. *Biophysical Journal* **63**, 215–233.

PLACE, J.F., SUTHERLAND, R.M. AND DAHNE, C. (1991). Opto-electronic immunosensors: a review of optical immunoassay utilizing immunomagnetic beads. *Analytical Chemistry* **64**, 1356–1361.

RAO, J., YAN, L., XU, B. AND WHITESIDES, G.M. (1999). Using surface plasmon resonance to study the binding of vancomycin and its dimer to self-assembled monolayers presenting D-Ala-D-Ala. *Journal of the American Chemical Society* **121**, 2629–2630.

SADANA, A. (1995). Antigen–antibody binding kinetics for biosensors: the fractal dimension and the binding rate coefficient. *Biotechnology Progress* **11**, 50–59.

SADANA, A. (1997). Binding kinetics for biosensor applications utilizing fractals: a categorization. *Journal of Colloid and Interface Science* **190**, 232–240.

SADANA, A. (1999). A single- and a dual-fractal analysis of antigen–antibody binding kinetics for different biosensor applications. *Biosensors and Bioelectronics* **14**, 515–531.

SADANA, A. AND BEELARAM, A. (1995). Antigen–antibody diffusion-limited binding kinetics of biosensors: a fractal analysis. *Biosensors and Bioelectronics* **10**, 301–316.

SADANA, A. AND MADAGULA, A. (1993). Binding kinetics of antigen by immobilized antibody or of antigen by immobilized antigen: influence of lateral interactions and a variable rate coefficient. *Biotechnology Progress* **9**, 259–269.

SADANA, A. AND MADAGULA, A. (1994). A fractal analysis of external diffusion-limited first-order kinetics for the binding of antigen by immobilized antibody. *Biosensors and Bioelectronics* **9**, 45–55.

SADANA, A. AND SII, D. (1992a). The binding of antigen by immobilized antibody: influence of a variable rate coefficient on external diffusion limitations. *Journal of Colloid and Interface Science* **151**, 166–177.

SADANA, A. AND SII, D. (1992b). Binding kinetics of antigen by immobilized antibody: influence of reaction order and external diffusional limitations. *Biosensors and Bioelectronics* **7**, 559–568.

SADANA, A. AND SUTARIA, M. (1997). Influence of diffusion to fractal surfaces on the binding

kinetics for antibody–antigen, analyte–receptor, and analyte–receptorless (protein) systems. *Biophysical Chemistry* **65**, 29–44.

SIGMAPLOT (1993). Scientific graphic software. User's manual. San Rafael, CA: Jandel Scientific.

SJOELANDER, S. AND URBANICZKY, C. (1991). Integrated fluid handling system for biomolecular interaction analysis. *Analytical Chemistry* **63**, 2338–2345.

SORENSON, C.M. AND ROBERTS, G.C. (1997). The prefactor of fractal aggregates. *Journal of Colloid and Interface Science* **186**, 447–452.

STENBERG, M. AND NYGREN, H.A. (1982). A receptor–ligand reaction studied by a novel analytical tool – the isoscope ellipsometer. *Analytical Biochemistry* **127**, 183–192.

STENBERG, M., STIBLERT, L. AND NYGREN, H.A. (1986). External diffusion in solid-phase immunoassay. *Journal of Theoretical Biology* **120**, 129–142.

STOCKLEY, P.G., BARON, A.J., WILD, C.M., PARSONS, I.D., MILLER, C.M., HOLTHAM, C.A.M. AND BAUMBERG, S. (1998). Dissecting the molecular details of prokaryotic transcriptional control by surface plasmon resonance: the methionine and arginine repressor proteins. *Biosensors and Bioelectronics* **13**, 637–650.

WILLIAMS, C. AND ADDONA, T.A. (2000). The integration of SPR biosensors with mass spectrometry: possible applications for proteome analysis. *TIBTECH* **18**, 45–48.